EUROPHYSICS LETTERS 15 March 2004

Europhys. Lett., **65** (6), pp. 823–829 (2004)
DOI: 10.1209/epl/i2003-10198-7

Current dependence of the magnetoresistance in a colloidal-sphere-masked ion-milled $La_{0.67}Sr_{0.33}MnO_3$ thin film

J. Li[1,2](*), D. N. Zheng[1], X. S. Rao[3], C. H. Sow[2], L. Chen[1] and C. K. Ong[2]

[1] *National Laboratory for Superconductivity, Institute of Physics Chinese Academy of Sciences - Beijing 100080, PRC*
[2] *Centre for Superconducting and Magnetic Materials (CSMM) and Department of Physics, National University of Singapore 2 Science Drive 3, Singapore 117542*
[3] *Temasek Laboratories, National University of Singapore Engineering Drive 3, Singapore 119260*

(received 11 August 2003; accepted in final form 8 January 2004)

PACS. 75.47.Gk – Colossal magnetoresistance.
PACS. 75.47.Lx – Manganites.
PACS. 72.25.Dc – Spin polarized transport in semiconductors.

Abstract. – An epitaxial $La_{0.67}Sr_{0.33}MnO_3$ thin film covered with a monolayer of colloidal spheres was ion-milled so that structural discontinuities were involved. Nonlinear V-I characteristics have been observed, revealing that the zero-field resistance of the sample decreases with increasing measuring current I. In a magnetic field, however, the resistance varies non-monotonically with I. An inflexion appears around $I = 50\,\mathrm{nA}$. Accordingly, the magnetoresistance also correlates with I. A maximum value as high as -700% ($\Delta R/R_H$) is recorded at liquid nitrogen in 1.5 T when $I = 1\,\mathrm{nA}$. The drastic current dependence of the magnetoresistance is believed to come from the ion-milling–induced structural and magnetic disorders and to be related to the inelastic scattering of the spin-polarized electrons at the disorders. The possible underlying mechanisms are discussed in detail.

In the past few years, the tremendous interest in the perovskite manganites has converted gradually to the investigation of *extrinsic* magnetoresistance (eMR) effects [1]. Appreciable low-field eMR has been discovered in systems with structural discontinuities, such as grain boundaries (natural [2] or artificial [3]), domain walls [4, 5], insulating second phases [6, 7], or dimension constrictions [8–10]. There have been a few reports on resistance change of as large as 500 percent in an applied field of only a few tens of Oersted [11]. The basic physical mechanism behind all these various phenomena appears to be the same, which is likely to be the spin-polarized tunnelling [1]. However, due to the diversity in geometry and the perhaps imperfect domain wall barriers, experiments yield a range of values and consensus has not been reached on either the sign or the magnitude of the eMR ratio. In this letter we present a

(*) E-mail: lijie@ssc.iphy.ac.cn

© EDP Sciences

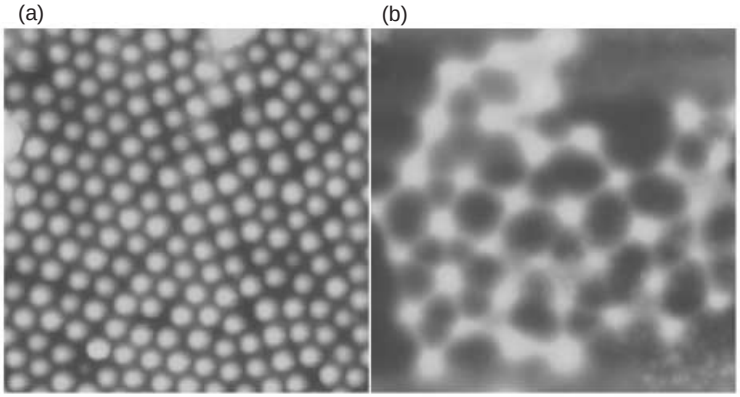

Fig. 1 – (a) AFM image of the SiO_2 spheres arranged on the $La_{0.67}Sr_{0.33}MnO_3$ film surface. The scale of the image is $10 \times 10\,\mu m^2$. The diameter of each sphere is $0.5\,\mu m$. (b) A part of the bridge after ion milling. The light regions are the residual LSMO film. The image scale is $5 \times 5\,\mu m^2$.

$La_{0.67}Sr_{0.33}MnO_3$ (LSMO) sample with a structural discontinuity induced by ion milling using a monolayer of colloidal spheres as the mask [12]. It shows nonlinear V-I dependence, which indicates that the zero-field resistance decreases monotonically with increasing measuring current I. It is found that the temperature dependence of the sample resistance also changes as measured with different I. Furthermore, the magnetoresistance (MR) increases drastically with decreasing I. As a result, in a field the resistance-current curve, read from the MR hysteresis loops measured with different I, shows an inflexion. The experimental observations can be understood by a combined effect of the current and magnetic field to the magneto-transport behavior at the magnetic domain walls.

The epitaxial LSMO thin film was grown on a (001)-$SrTiO_3$ substrate by pulsed-laser deposition (PLD) [13,14]. The film was first patterned using conventional wet-etching technique to form a bridge of $30\,\mu m$ in width and $50\,\mu m$ in length. After the photoresist was completely removed by acetone, a droplet of colloid with SiO_2 spheres of diameter $0.5\,\mu m$ was let fall onto the film near the bridge area. The film was then set to spin in a preset speed to spread the colloidal spheres on the film surface, and then put in air at room temperature for 24 hours to desiccate. The bridge area covered with spheres was then checked by atomic force microscopy (AFM) to ensure that there is only one single layer of spheres stacked. The ion milling was carried out using the Oxford Scientific Plasma (OSPrey) Source power supplied by an Advanced Energy RFX-600. Another set of mask was adopted to protect areas other than the bridge. The rf power used was 400 W and the accelerating voltage 500 V. The sample was cooled by liquid nitrogen during the whole milling process. The milling process was deliberately interrupted for several times and the film was moved out from the chamber for complete transport property measurements. The milling was continued till a resistance value higher than $50\,k\Omega$ was obtained, meaning that only a few percolation paths exist. The magneto-electrical properties of the bridge were measured using the four-probe method in an applied magnetic field up to 1.5 tesla, parallel to the current direction.

Figure 1(a) is the AFM observation of the colloidal spheres on the LSMO film surface. In this $10 \times 10\,\mu m^2$ region, the SiO_2 spheres are almost closely arranged on the films surface, without serious overlapping, although some defects such as "dislocations" or "grain boundaries" exist. These spheres act very well as a mask during the ion milling, as can be clearly seen in fig. 1(b). The core area under each sphere forms an island, and the film among three

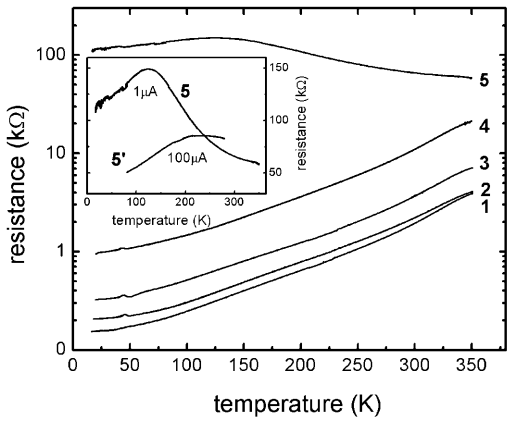

Fig. 2

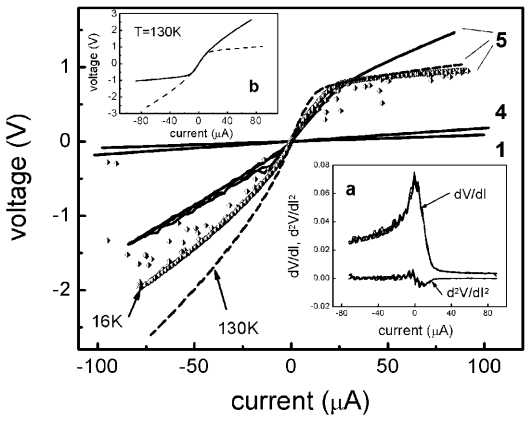

Fig. 3

Fig. 2 – *R-T* curves of the bridge measured before (denoted as number 1), and after different periods of ion milling (denoted sequentially by numbers 2-5). The inset shows the *R-T* curves of the sample finally obtained (number 5), measured with different currents, 1 μA and 100 μA.

Fig. 3 – *V-I* dependencies of the bridge before and after different periods of ion milling (as denoted by numbers), measured at 300 K if not indicated. Inset a shows the differentiations of the dashed line. Inset b presents the curve measured with a configuration different from that of the dashed line.

spheres is totally etched off. A narrow conducting path then appears in between two islands due to the shade effect. The length of each patch is no more than 0.3 μm and the width less than 50 nm, noting that the scale for this image is $5 \times 5\,\mu\mathrm{m}^2$. We have to admit that there are still small areas that have not been covered with spheres, which were fully exposed to the ion radiation afterwards, and thus are completely etched off. With increase of the milling time, the out-of-plane dimension of these pathes reduces, and fewer and fewer of these pathes survive, which finally form a broken 2D conducting network. A spin-polarized electron then must hop through these links to each knot when a current is supplied. We consider these narrow links as a kind of structural discontinuities in the film, which consists of both dimension constrictions and lattice defects caused by ion radiation.

After each milling stage, the temperature dependence of the bridge resistance was measured and all the results are shown in fig. 2. The curves are denoted by numbers 1-5, representing different ion-milling stages. It is clear that, before ion milling, the bridge behaves like a metal in the temperature range measured, with its insulator-to-metal (I-M) transition temperature higher than 350 K. The curve can be well fitted by $R = R_0 + R_2 * T^2 + R_{4.5} * T^{4.5}$, which suggests that the resistance comes from both the single-magnon scattering and the two-magnon scattering process [15], and thus the conducting electrons in this sample is not fully spin-polarized, at least at a regime near the ferromagnetic transition temperature T_c. This is the reason why we carried all the MR measurements mentioned below at liquid nitrogen. With ion milling, part of the films was etched off and the resistance increases. The *R-T* curve keeps the similar shape as the original one, until finally the room temperature resistance of the sample reaches to $\sim 60\,\mathrm{k}\Omega$, and an I-M transition appears around 130 K. Careful investigation shows that, as presented in the inset of fig. 2, this *R-T* dependence (denoted by number 5 in the figure) varies as measured with different I. When I was increased from 1 μA to 100 μA, the resistance measured reduced and the I-M transition right-moved, suggesting a nonlinear *V-I* characteristic

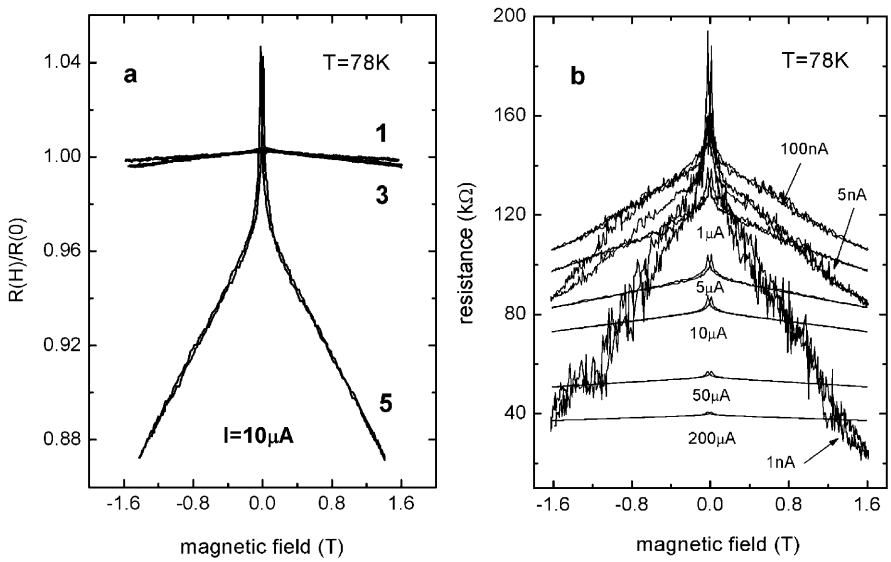

Fig. 4 – (a) Resistance changes of the bridge, before and after different ion-milling stages as denoted, in a sweeping magnetic field up to 1.5 T at 78 K. (b) The resistance *vs.* the applied magnetic field loops at 78 K for the bridge after the final milling stage (number 5), measured with different currents ranging from 1 nA to 200 μA.

of the bridge. It appears that the metallic conducting behavior of the sample was partially recovered as measured with a larger current. Here the thermal effect could be ruled out because asymmetric V-I characteristics have been observed, as will be detailed in the following.

Shown in fig. 3 are the V-I curves of the bridge measured before and after different periods of milling. Numbers in the figure represent ion-milling stages, consistent with those in fig. 2. Before ion milling, the V-I curve of the bridge at room temperature is linear, complying Ohm's law. As the milling duration prolongs, the resistance of the sample rises and the slope of the V-I curve increases. Finally, the curve becomes nonlinear. The nonlinear dashed line and the line labelled by shaded diamonds are measured for the sample after the final milling stage at 130 K and 16 K, respectively. The nonlinearity increases with decreasing temperature. The first- and second-order differentiations of the V-I curve measured at 130 K are shown in inset a of the figure. One may note that the nonlinearity is significantly asymmetric for positive and negative currents. Reversing the direction of the input current and simultaneously swapping the voltage measurement electrodes led to a curve symmetric to the origin of the coordinate with the previous one, as shown in inset b of fig. 3. This indicates that the asymmetry of the V-I curve is originated from the sample itself, instead of from the measurement configuration. The asymmetric V-I curves also help to retort the thermal-effect explanation to the inset of fig. 2. Finally, the curve measured at 16 K exhibits considerable fluctuations. A number of experimental points with very low resistance stick out from the curve. This is a hint that avalanches occur in some instance at this temperature, which may originate from the unique geometry of our device, where many narrow links exist.

Nonlinear V-I characteristics have been observed in many ferromagnetic nanocontacts, such as Ni [9], Fe_3O_4 [11], and $La_{0.67}Sr_{0.33}MnO_3$ [16], or more generally in some ferromagnetic systems with regions of depressed structural and magnetic ordering [17]. For the nanocontacts, it is argued that the nonlinearity may be due to the "magnetic balloon effect" of the

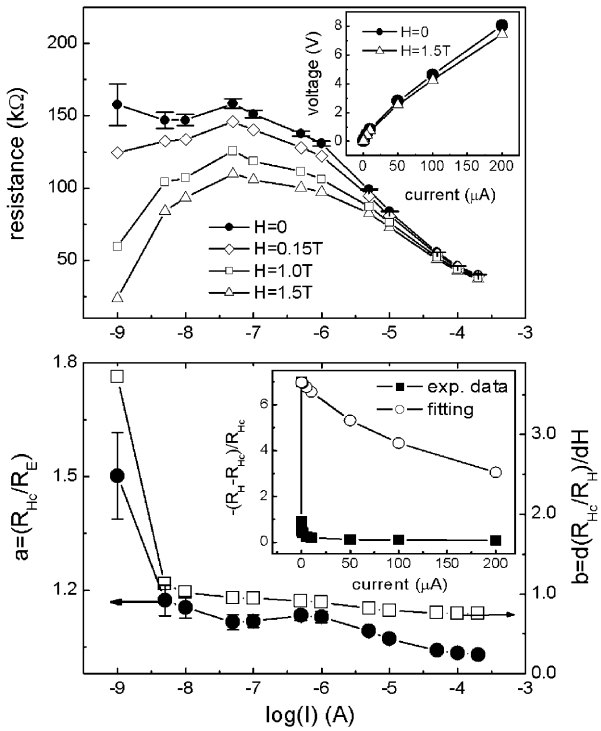

Fig. 5 – Top panel: sample resistance measured with different I at $H = 0$, 0.15, 1.0, and 1.5 T, read from fig. 4(b). The inset shows the V-I curves at $H = 0$ and 1.5 T, also restored from fig. 4(b). Bottom panel: $\ln I$-dependence of the low-field resistance ratio (a), and the high-field slope (b). Here $R_{\rm E}$ is the intercept as extrapolating the high-field linear part to the resistance axis. The inset shows the $-(R_{Hc} - R_H)/R_H$ values measured at different I, and the calculated results if considering only the effect of inelastic scattering.

domain wall at the geometry constrictions [11]. For the latter, Hofener *et al.* [17] have given a reasonable explanation based on inelastic scattering of the spin-polarized conducting electrons at a barrier.

To reveal the magneto-transport mechanisms in our sample, after each milling stage we also recorded the magnetic-field dependence of the bridge resistance. Shown in fig. 4(a) are three of the curves recorded at 78 K with a measuring current 10 μA. Before ion milling (number 1), the bridge resistance changes linearly with the applied magnetic field, indicating a good crystallinity of the film. With ion milling (number 3) the curve slope rises, and two small shoulders appear at the vicinity of coercive fields. After the final milling stage, the curve shows clear two-segment feature and greatly enhanced $\Delta R/R$ ratio, suggesting an extrinsic MR. Shown in fig. 4(b) are the resistance *vs.* field loops for the bridge after the final milling stage, measured with different currents. Perfect butterfly-shaped loops were obtained for each measuring current, except that the noise increases when the measuring current and thus the voltage signal is reduced. It is attracting that the MR ratio decreases drastically with increasing measuring current. As $I = 1$ nA, the bridge exhibits MR as high as -700% if defined as $(R_{Hc} - R_H)/R_H$, where R_{Hc} is the resistance at the shoulders of the curve. The value is only -9% as $I = 200\,\mu$A. The measurement has been repeated for a couple of times later and the observation was roughly the same, except that the zero-field resistance increased

gradually with time due to the decay of the sample. The observed remarkable dependence of eMR on the measuring current is unusual and worth of much attention.

Resistances are read from the loops for various measuring currents at $H = 0, 0.15, 1.0,$ and 1.5 T. The results are re-plotted as R-I relations in the top panel of fig. 5. From these data, V-I curves at $H = 0$, and 1.5 T are also restored and plotted as in the inset, which is consistent with the nonlinear V-I curves previously observed. Their smoothness may also help to verify the reliability of our experimental data. At the high current end, as can be seen from the top panel, the zero-field resistance of the bridge seems to decrease exponentially with increasing current. As the current is lower than 50 nA, the resistance tends to be saturated. When a magnetic field is present, however, the resistance show a maximum at $I = 50$ nA, and drops again as the current is further reduced.

In order to reveal the origin of the extremely large MR change as measured with different I, we borrow Lee's classification and rewrite the extrinsic MR ratio into two parts [18]:

$$\frac{\sigma}{\sigma_0} - 1 = \frac{R_0 - R_H}{R_H} = (a-1) + bH, \tag{1}$$

where $(a-1)$ is the nonlinear low-field MR coming from the magnetic domain rotation in a field, and bH is the linear high-field part due to the alignment of the originally weakly localized spins. Plotted in the bottom panel of fig. 5 are the data at 1.5 T for different measuring currents. Here we use R_{Hc} to replace R_0 in eq. (1). Careful investigation reveals that although the values of a are scattering with relatively large error bar at low currents, its trend of rising with decreasing I is still clear. $a-1$ rises from 3% to 50% as I decreases from 200 μA to 1 nA. Meanwhile, the slope b also rises steadily and drastically with decreasing I, which is apparently the main reason for the extremely large MR ratio measured at small I. We note that the value b in our experiment is fairly high, all above 0.75 with a maximum value of 3.7, as compared with the data of 0.16 in polycrystalline bulks [18]. This implies that the spin disordering at the bridge area is different from that at an ordinary grain boundary. Apparently, at the bridge there are a large number of weakly localized spins that can be aligned in a relatively low magnetic field. We believe that these spins are pinned by the high density of lattice defects induced by ion bombing. It is then also reasonable to suggest that the domain walls at the bridge which are dressed with lattice defects are not "pure". In this case, according to Höfener *et al.* [17], inelastic scattering of the originally spin-polarized electrons through localized defect states will occur.

With increase of the measuring current I, inelastic tunnelling contributes more and more to the charge transport across the bridge, which can be the reason of the nonlinear V-I curves observed. Since spin polarization may not be conserved in the inelastic scattering, the inelastic tunnelling current does not contribute to the magnetoresistance and the measured eMR ratio reduces accordingly, following [17]

$$\triangle R/R_H(I) = \frac{I_e}{I}(I) \cdot \triangle R/R_H(I_{e0}), \tag{2}$$

where I_e is the current for the elastic channel. From the zero-field V-I curve shown in the top inset of fig. 5, we determined the ratio I_e/I as a function of I, and took the MR value measured at $I = 1$ nA as $\triangle R/R_H(I_{e0})$. While the calculated MR value does decrease considerably with I, its change is much milder than that of the experimental data, as shown in the bottom inset of fig. 5.

Therefore, our experimental observation cannot be fully attributed to the electron inelastic scattering. A second mechanism must exist, especially at lower $I < 50$ nA, where a steep MR drop occurs but inelastic scattering is ignorable. It is the co-play of the two mechanisms that

accounts for the inflexion on the $R-I$ relation in a field. The second mechanism may be the magnetic balloon effect, where the domain walls drift and expand under the spin pressure of the conducting electrons [11]. However, since the dimension information about our device is somewhat vague, strong evidence supporting this assumption is still lacking. Furthermore, it still cannot explain the sharp drop of R_H at extremely low I. Another possibility may come from the unique geometric structure (the broken network) at the bridge. Further experiment is necessary to clarify this issue.

In summary, we have introduced structural discontinuities into a $La_{0.67}Sr_{0.33}MnO_3$ thin film by ion milling. Nonlinear V-I curves and a great dependence of MR ratio on the measuring current have been observed. While inelastic scattering can be one of the underlying mechanism, another mechanism gets in at low current regime, which is currently unknown.

* * *

This work is partially supported by the National Natural Science Foundation of China under grant No. 10174093, and the Ministry of Science and Technology under Grant No. NKBRSF-G19990646.

REFERENCES

[1] Ziese M., *Rep. Prog. Phys.*, **65** (2002) 143.
[2] Coey J. M. D., *J. Appl. Phys.*, **85** (1999) 5576.
[3] Mathur N. D., Burnell G., Isaac S. P., Jackson T. J., Teo B. S., MacManus-Driscoll J. L., Cohen L. F., Evetts J. E. and Blamire M. G., *Nature*, **387** (1997) 266.
[4] Yamanaka N. and Nagaosa N., *J. Phys. Soc. Jpn.*, **65** (1996) 3088.
[5] Mathur N. D., Littlewood P. B., Todd N. K., Isaac S. P., Teo B.-S., Kang D.-J., Tarte E. J., Barber Z. H., Evetts J. E. and Blamire M. G., *J. Appl. Phys.*, **86** (1999) 6287.
[6] Petrov D. K., Krusin-Elbaum L., Sun J. Z., Feild C. and Duncombe P. R., *Appl. Phys. Lett.*, **75** (1999) 995.
[7] Liu J.-M., Li J., Huang Q., You L. P., Wang S. J., Ong C. K., Wu Z. C. and Liu Z. G., *Appl. Phys. Lett.*, **76** (2000) 2286.
[8] García N., Muñoz M. and Zhao Y.-W., *Phys. Rev. Lett.*, **82** (1999) 2923.
[9] García N., Rohrer H., Saveliev I. G. and Zhao Y.-W., *Phys. Rev. Lett.*, **85** (2000) 3053.
[10] Bruno P., *Phys. Rev. Lett.*, **83** (1999) 2425.
[11] Versluijs J. J., Bari M. A. and Coey J. M. D., *Phys. Rev. Lett.*, **87** (2001) 026601.
[12] Hoogenboom J. P., Vossen D. L. J., Faivre-Moskalenko C., Dogterom M. and Blaaderen A. V., *Appl. Phys. Lett.*, **80** (2002) 4828.
[13] Li J., Ong C. K., Liu J.-M., Huang Q. and Wang S. J., *Appl. Phys. Lett.*, **76** (2000) 1051.
[14] Zhan Q., Yu R., He L. L., Li D. X., Li J., Xu S. Y. and Ong C. K., *Phys. Rev. Lett.*, **88** (2002) 196104.
[15] Salamon M. B. and Jaime M., *Rev. Mod. Phys.*, **73** (2001) 583.
[16] Versluijs J. J., Bari M., Ott F., Coey J. M. D. and Revcolevschi A., *J. Magn. & Magn. Mater.*, **211** (2000) 212.
[17] Höfener C., Philipp J. B., Klein J., Alff L., Marx A., Büchner B. and Gross R., *Europhys. Lett.*, **50** (2000) 681.
[18] Lee S., Hwang H. Y., Shraiman B. I., Ratcliff II W. D. and Cheong S.-W., *Phys. Rev. Lett.*, **82** (1999) 4508.